Revista Brasileira de Geografia Física

ISSN:1984-2295

Homepage: https://periodicos.ufpe.br/revista

Validation of Double Constant and Falling Head Permeameter for Determination of Hydraulic Conductivity of Soils in the Laboratory

Brivaldo Gomes de Almeida[1], Edson Marlon da Silva Santos[2], Fernando José Freire[3], Ceres Duarte Guedes Cabral de Almeida[4], Talmo Henrique dos Santos Silva[5], Ana Lua Telles Lima[6], Jaedson Cláudio Anunciato Mota[7]

[1]Associate Professor at UFRPE, CEP: 52.171-900, Recife (PE), Brazil, Tel.: (+55 81) 997155416, brivaldo.almeida@ufrpe.br (corresponding author); [2]Master in Soil Science from the Federal Rural University of Pernambuco (UFRPE), CEP: 52.171-900, Recife (PE), Brazil, Tel.: (+55 81) 99834-2958, edsonmarlonagro@gmail.com; [3]Full Professor at UFRPE, CEP: 52.171-900, Recife (PE), Brazil, Tel.: (+55 81) 98230-0026, fernando.freire@ufrpe.br; [4]Full Professor at Agricultural College Dom Agostinho Ikas (CODAI), UFRPE, CEP: 54.730-970, São Lourenço da Mata (PE), Brazil, Tel.: (+55 81) 997155411, ceres.cabral@ufrpe.br; [5]Doctoral student of the Postgraduate Program in Soil Science at UFRPE, CEP: 52.171-900, Recife (PE), Brazil, Tel.: (+55 81) 98597-8514, talmo.henrique@hotmail.com; [6]Master in Environmental Engineering from UFRPE, CEP: 52.171-900, Recife (PE), Brazil, Tel.: (+55 81) 98597-8514, analua.lima@gmail.com; [7]Associate Professor at the Federal University of Ceará (UFC), CEP: 60.440-554, Fortaleza (CE), Brazil, Tel.: (+55 85) 98719-9808, jaedson.mota@ufc.br

Artigo recebido em 08/11/2023 e aceito em 08/11/2024

A B S T R A C T

The objective of this research was to validate alternative equipment for determining the hydraulic conductivity of saturated soil (K_{sat}) in laboratory settings. The aim was to develop a single piece of equipment that could be used to carry out tests using both the constant-head permeameter (CHP) and the falling-head permeameter (FHP) methods with minimal disturbance to the samples. To this end, undisturbed soil samples were collected (in volumetric cylinders with 100 and 250 cm^3) from three soil profiles with different textures to evaluate the sensitivity of the double permeameter (DP) in determining K_{sat}, considering the method, the sample size, and the textural class of the soils. To assess the efficacy of the DP in estimating Ks_{at}, the coefficient of variation (CV) was determined for the two methods (CHP and FHP), the sample size (100 and 250 cm^3), and the applied hydraulic head (cwc) (constant: 1.5 and 2.5 cwc; falling: Δh_i, upper limit, h_1 = 67.6 and h_2 = 57.6 cwc; Δh_{ii}, medium limit, h_1 = 49.3 and h_2 = 39.3 cwc; and Δh_{iii}, lower limit, h_1 = 31.3 and h_2 = 21.3 cwc). The results indicate that the DP may be employed as an alternative permeameter for K_{sat} tests employing the CHP and FHP methods. The most favorable statistical coefficients were observed in tests conducted with samples of a sandy texture (Profile 3, Ap horizon), particularly those with a larger volume (250 cm^3), for both the CHP and FHP methods, irrespective of the applied hydraulic head. The equipment can be utilized within the full range of methodological limits employed in this study, and the appropriate limit must be selected according to the physical properties of the soil to be employed in the tests.

Keywords: permeability, preferential flow, Darcy’s equation, soil water dynamics.

Validação de Permeâmetro Duplo de Carga Constante e Descendente para Determinação de Condutividade Hidráulica de Solos em Laboratório

R E S U M O

Esta pesquisa objetivou validar um equipamento alternativo para determinação da condutividade hidráulica do solo saturado (K_{sat}) em laboratório, onde, num único equipamento, foi possível realizar ensaios pelos métodos do permeâmetro de carga constante (CHP) e/ou permeâmetro de carga decrescente (FHP), com mínima perturbação da amostra. Para isso, foram coletadas amostras não deformadas de solos (cilindros volumétricos, com 100 e 250 cm^3) em três perfis de solos, com diferentes texturas, para avaliar a sensibilidade do permeâmetro duplo (DP) na determinação da K_{sat} em função do método, tamanho da amostra e classe textural dos solos. Para avaliar o desempenho do DP em estimar a K_{sat}, foi calculado o coeficiente de variação para os

dois métodos (CHP, FHP), o tamanho da amostra (100 e 250 cm^3) e as cargas hidráulicas aplicadas (constante: 1,5 e 2,5 cca; decrescente: Δh_i: limite superior, h_1 = 67,6 e h_2 = 57,6 cca; Δh_{ii}, limite médio, h_1 = 49,3 e h_2 = 39,3 cca; e Δh_{iii}, limite inferior, h_1 = 31,3 e h_2 = 21,3 cca). Os resultados sugerem que o DP pode ser usado como permeâmetro alternativo para os ensaios de Ksat pelos métodos do CHP e FHP. Os melhores coeficientes estatísticos foram observados para os ensaios com as amostras de textura arenosa (Perfil 3, horizonte Ap), principalmente aquelas de maior volume (250 cm^3), tanto para o CHP como para o FHP, independentemente da carga hidráulica aplicada. O equipamento pode ser manuseado em todos os limites metodológicos aplicados nesse estudo, devendo ser selecionado o limite de acordo com as propriedades físicas do solo a ser utilizado nos ensaios.
Palavras-chave: permeabilidade, fluxo preferencial, equação de Darcy, dinâmica da água no solo.

Introduction

Hydraulic conductivity is a soil property that represents the ease with which water permeates its pore spaces (Ferdinand et al., 2023). The maximum value of hydraulic conductivity is reached when the soil is saturated and is therefore defined as the hydraulic conductivity of the saturated soil, denoted K_{sat} (Guedessou et al., 2021).

Therefore, the study of this hydraulic property of the soil is of great importance for understanding the behavior of water dynamics in the soil. Furthermore, it can be applied to increase the efficiency of agricultural management in terms of fertilization, irrigation, and drainage (Gootman et al., 2020).

The methods for determining K_{sat} are distinguished by varying degrees of precision and are selected according to soil texture. These methods are typically classified into two categories: direct and indirect. In direct methods, K_{sat} is obtained through tests that directly measure the water flow in a specimen, both in the laboratory and *in situ* (Su et al., 2020; Nam et al., 2021). Conversely, in indirect methods, K_{sat} is estimated by equations, called pedotransfer functions, constructed from other soil properties (Feki et al., 2020).

In the field, the Guelph permeameter is one of the most commonly used methods. In laboratory settings, the constant-head permeameter (CHP) and the falling-head permeameter (FHP) are the most prevalent methods (Liao et al., 2022; Yan et al., 2024). The selection of a particular method is contingent upon the permeability coefficient of the soil. The CHP method is recommended for soils with greater permeability, such as those with a sandier texture, where macropores are prevalent. Conversely, the FHP method is recommended for soils with a more clayey texture, where micropores are the dominant feature (Liu et al., 2022; Solangi et al., 2024).

The utilization of direct methods in testing may give rise to complications associated with air entrapment, which occurs when the specimen is saturated, particularly in field tests (Nam et al., 2021). Moreover, direct methods (field or laboratory) have additional drawbacks, including the necessity for costly equipment (Ferdinand et al., 2023) and the difficulty of employing both types of permeameter (CHP and FHP) in a single specimen with minimal disturbance, in addition to the time-consuming nature of the tests (Nam et al., 2021; Snoussi et al., 2024).

As Reynolds et al. (2000) observed, K_{sat} is highly sensitive to sample size and the specifics of the sampling procedures, flow geometry, and other factors. Moreover, the majority of existing methods are not universally applicable or accurate across all soil types (Nam et al., 2021).

Accordingly, the minimization of these disadvantages must be considered in the development of an alternative permeameter for determining K_{sat}. This may entail the interspersing of the application mode of the hydraulic head (constant or falling), the test time reduction, the use of a limited number of devices for its construction, the optimization of water usage, and, most importantly, the maintenance of the original structure of the soil sample. This approach is necessary to ensure the generation of accurate and representative results that reflect the actual soil conditions (Gubiani et al., 2010).

The objective of the present study was to validate a laboratory permeameter that could be used to determine K_{sat} using the CHP and FHP methods in a single test specimen, with minimal disturbance to the soil samples, to generate accurate and precise data, while also addressing the limitations of the equipment currently utilized.

Materials and Methods

Experimental site and selection of soil profiles

The research was conducted using soil samples collected from two distinct locations in the northeastern region of Brazil. Both sites are situated within the state of Pernambuco (PE). One is located at the Itapirema Experimental Station of the Instituto Agronômico de Pernambuco (IPA). This site is positioned along the banks of BR 101 Norte at km 53, Goiana (PE). The second site is situated at the José Ermírio de Morais Campus, which is part of the Dom Agostinho Ikas Agricultural College (CODAI), in Tiúma, São Lourenço da Mata (PE). In these areas, three locations were selected for soil profile opening, to avoid locations presenting preferential water flow in the soil pores, such as cracks or anthills. Profiles 1 and 2 were opened on the CODAI Campus, while Profile 3 was opened on the IPA. Following profile opening, morphological descriptions were carried out to obtain soil classifications (Table 1), following the Brazilian Soil Classification System (SiBCS), as proposed by Santos et al. (2018).

Table 1. Characteristics of the soils used to measure K_{sat} using permeameters (proposed and conventional).

Profile / Soil taxonomy*		Horizon	Depth (cm)	Soil bulk density (Mg m^{-3})	Textural Class
1	Argissolo Amarelo eutrocoeso abrupto	Ap	0-15	1.33	Sandy loam
		Bt_1	15-29	1.54	Clay loam
2	Argissolo Vermelho-Amarelo Distrocoeso típico	Ap	0-12	1.45	Sandy clay loam
3	Argissolo Amarelo distrocoeso epiáquico	Ap	0-14	1.41	Sandy
		Bt_1	42-70	1.67	Sandy clay loam

***Brazilian Soil Classification System – SiBCS (Santos et al., 2018)

Collection and volume of soil samples

In the selected profiles and horizons (Table 1), structured soil samples were collected using volumetric cylinders that were inserted into the soil with the aid of a Uhland-type sampler. This method was employed to maintain the soil structure with minimal disturbance, thereby ensuring the integrity of the K_{sat} trials.

To evaluate the performance of the double permeameter depending on the sample size, two volumes were tested (FAO, 2023). The first, referred to as the standard size, had a height and internal diameter of 5 cm (≅ 100 cm^3), while the second had a height and internal diameter of 5 cm (250 cm^3). The samples (cylinder-sample sets) were packaged with due care, using plastic film and bubble wrap, and placed in Styrofoam boxes to ensure the structural integrity of the samples during their transport to the Soil Physics Laboratory (LAFIS) of the Agronomy Department of the Federal Rural University of Pernambuco (UFRPE), Recife, Pernambuco State, Brazil. The cylinder-sample sets were reserved for K_{sat} determination tests.

Tests of physical characterization of the soils

In addition to the K_{sat} tests, the cylinder-sample sets were employed to ascertain other attributes contingent upon the maintenance of the soil structure. This included soil bulk density (Bd, in Mg m^{-3}), which was determined via the volumetric cylinder method (Grossman and Reinsch, 2002), and total porosity (TP, in %), which was determined via the saturation method (Reichert et al., 2021), whereby it was assumed that the pore volume (V_{pores}) equaled the volume of water required to saturate the pores, and the soil volume (V_{soil}) was equal to the volume of the cylinder used to collect soil. The soil volume was then calculated via equation (1).

$$TP_{(\%)} = \left(\frac{V_{pores}\ (cm^3)}{V_{soil}\ (cm^3)}\right) \times 100 \quad (1)$$

Unstructured samples were utilized in characterization tests that do not require the maintenance of the sample structure, such as the “f” factor and granulometric analysis. These samples were collected via auger and subsequently converted to air-dry fine earth (ADFE) in the laboratory. This process involved the crumbling and sieving of the samples through 2-mm mesh openings, resulting in the formation of air-dried samples.

The soil particle size analysis was conducted using the hydrometer method, initially proposed by Gee and Or (2002) with modifications commented below. Total clay (TC) was determined with just one reading on the hydrometer (ASTM 152 H), after clay dispersion and 24 hours of rest from manual agitation, with total sand (TS) and its subfractions obtained by sieving. The silt fraction was calculated considering equation (2)

$$Silt_{(\%)} = 100 - (TS_{\%} + TC_{\%}) \quad (2)$$

Additionally, the amounts of water-dispersible clay (WDC) were determined, and the clay flocculation degree (FD) and the clay dispersion degree (DD) were calculated according to equations (3) and (4), respectively.

$$FD_{(\%)} = \left(\frac{TC - WDC)}{TC}\right) \times 100 \quad (3)$$

$$DD_{(\%)} = 100 - FD \quad (4)$$

Additionally, the ADFE samples were employed to ascertain the soil particle density (Pd, in Mg m^{-3}) through the utilization of the pycnometer method (Flint and Flint, 2002).

These properties were determined to ascertain the K_{sat} behavior in each horizon under examination and to elucidate the impact of this behavior on the outcomes of the K_{sat} tests, as proposed by Ferdinand et al. (2023).

The number of samples utilized in the tests was calculated based on the high variability of K_{sat}, which is determined by its coefficient of variation (CV), which is higher in comparison to the soil properties that influence K_{sat}, which exhibit less variability (Reichert et al., 2021).

Double permeameter: construction details and specifications

The double permeameter (DP) utilized in this investigation was the subject of an invention patent with the National Institute of Industrial Property (INPI) under the number BR 10 2020 013202 4 (Almeida et al., 2020).

The DP was developed at LAFIS at UFRPE based on NBR 13292 of the Brazilian Association of Technical Standards (ABNT) as an alternative permeameter for K_{sat} determination tests in the laboratory. The DP is comprised of a cylindrical container, constructed from a nylon billet, which can be utilized with a variety of materials, including plastic and acrylic. The billet is processed on a mechanical lathe to create a concentric hole with a diameter sufficient to accommodate a test body (sample cylinder) within. At the lower end of the container, a threaded nipple (Figure 1) is present, where the fluid drain hose is attached.

In the upper section of the container, four screws were installed with butterfly nuts, which serve to guide and fix the lids. The upper lid 1 is UL1 (Figures 1B and 2A), and the upper lid 2 is UL2 (Figures 1F and 2B). UL1 is employed to ascertain K_{sat} through the constant-head permeameter (CHP) method, whereas UL2, equipped with a nipple, is dedicated to the falling-head permeameter (FHP) method, enabling the head application mode to be alternated. This is achieved by simply replacing the exclusive cap for each method, without disturbing the sample cylinder, allowing for the utilization of either hydraulic constant or falling modes.

The sealing rubber is situated within the internal base of the DP (Figure 2C), followed by the containment plate (Figure 2D), in which the sample cylinder is positioned (Figure 2E).

In the upper portion of the cylinder-sample, an additional containment plate and a second rubber seal are inserted, as illustrated in Figures 1B and 1F. Subsequently, the upper lid is placed (Figures 2A or 2B) and the nuts are placed on the screws, which serve to adjust and seal the entire assembly (Figures 1C and 1G), thereby allowing the liquid to flow only through the pores of the test piece.

Determination of K_{sat}: procedures and methodological limits

Once the permeameters have been assembled (Figures 1C/1D and 1G/1H), the next step is to select the method for determining the K_{sat} value in the laboratory. This can be either the CHP or FHP method. Regardless of the method chosen, the initial procedure is sample saturation (sample cylinder), as illustrated in Figure 3A. It is recommended that deaerated water (boiled and cooled under vacuum to room temperature) be used to fill the soil pores from the bottom to the top slowly (Figure 3A) to avoid air entrapment in the pores during saturation. The saturation process is deemed complete when a water lens is observed on the surface of the sample. This lens will appear mirrored and can be tested by reflecting light (for example, from a flashlight) directed at the sample surface. Subsequently, if the CHP method is selected, the Mariotte bottle is employed to maintain a constant hydraulic head (h) on the specimen. This height is variable, ranging from 1 to 5 cm (Figure 3B), contingent on the soil permeability. Accordingly, it is recommended that higher heights be employed for soils exhibiting low permeability. In these soils, K_{sat} tests can be conducted with the h setting, simply modifying the height of the Mariotte bottle within the UL1 lid (Figures 2A and 3B). Consequently, in the K_{sat} tests conducted via the CHP method, each cylinder-sample set (100 and 250 cm^3) was subjected to the application of a constant hydraulic head (h), after which the water volume (Wv) permeated through the area was collected. This was done to obtain the Wv permeated through the cross-section of the specimens (Figure 3B), in a fixed time interval (t), until the flow rate (Wv/t) reached a constant value (Reynolds and Elrick, 1986), a condition that was defined when three or four consecutive measurements exhibited differences of ≤ 5% (Liu et al., 2022).

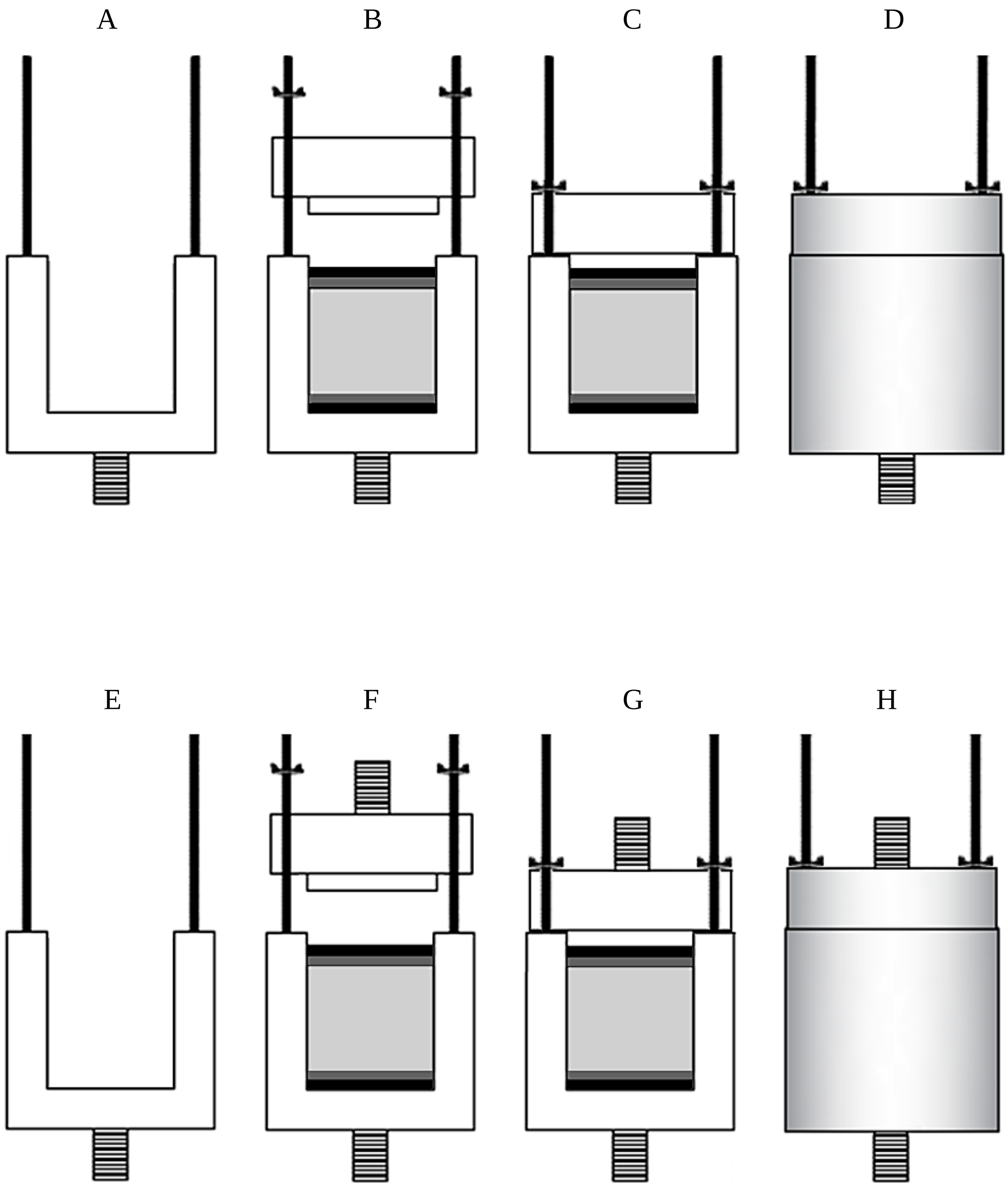

Figure 1. Details of the double permeameter (DP) and its parts, for saturated hydraulic conductivity tests depending on the applied hydraulic head, where A, B, C, and D, method under constant-head permeameter (CHP), and E, F, G and H, method with falling-head permeameter (FHP).

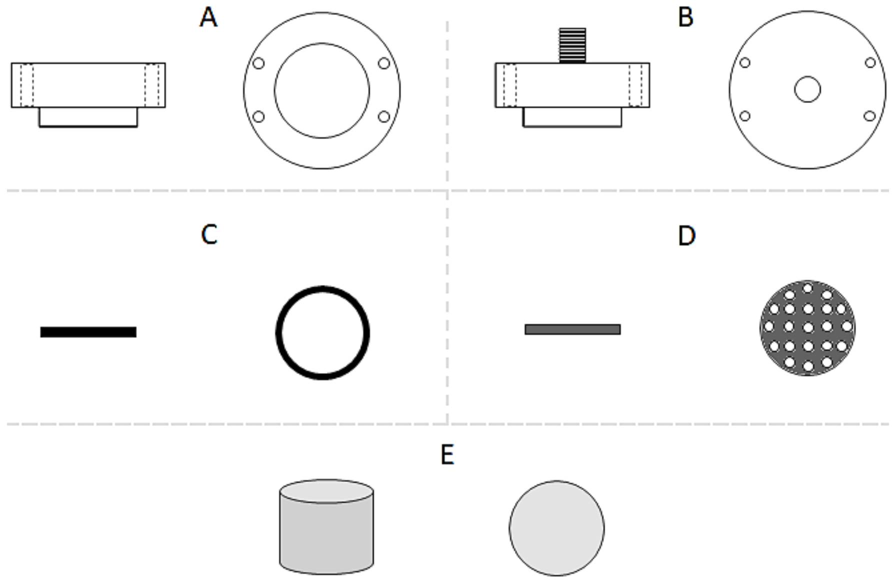

Figure 2. Parts of the double permeameter (DP) with specificities in: A) upper lid 1 (UL1), for the constant-head permeameter method; B) upper lid 2 (UL2), falling-head permeameter method; C) specimen containment plate; D) sealing rubber; E) volumetric cylinder for collecting and containing the specimen (sample holder). In the figures, the devices on the left represent the side view, while those on the right exhibit the top view.

In the case of tests that require the use of the FHP method, the UL1 lid is replaced by the UL2 lid (Figure 2B), which is connected to a graduated glass tube, burette type, using a silicone hose (Figure 3C). Two points are marked on the burette, where the heights (h_1 and h_2) are measured in relation to the reference level (RL). Thus, the hydraulic head (h) varies in a decreasing manner between h_1 and h_2, which are heights referring to the upper and lower limits, respectively, and measuring the time that the meniscus of the water column passes between them (Δt).

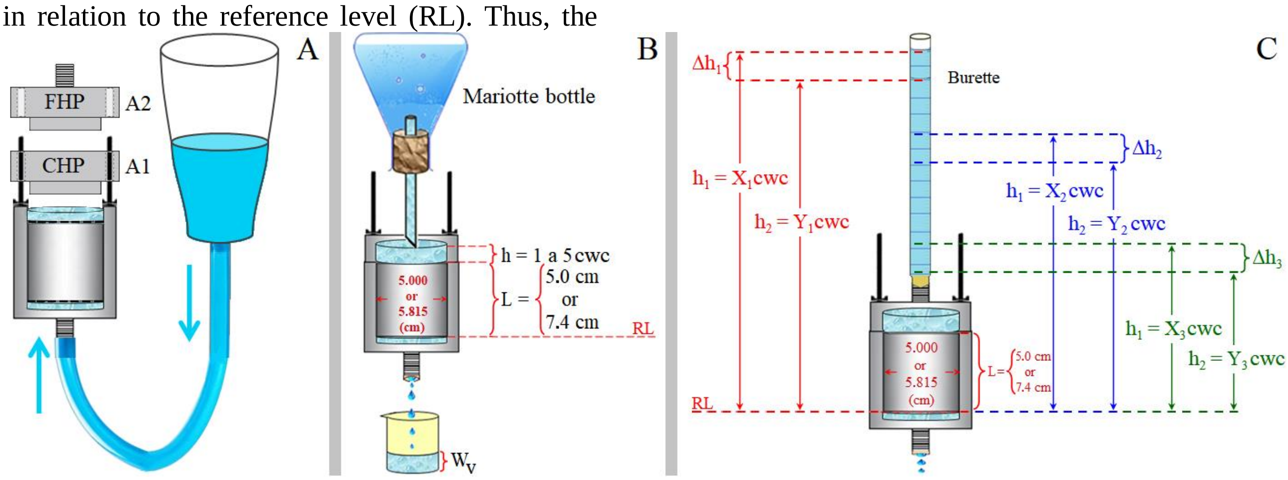

Figure 3. Proposed permeameter for K_{sat} tests, with details for: A) saturation of the specimen (A1, with the upper lid 1 – UL1, for tests via constant-head permeameter – CHP; and A2, with the upper lid 2 – UL2, in the case of using the falling-head permeameter – FHP; B) CHP method; C) FHP method, with variations between h_1 and h_2 (Δh_1, Δh_2, and Δh_3). The figures do not maintain proportions to each other.

Accordingly, the distance between heads h_1 and h_2 (Δh) can be modified in relation to the reference level, allowing for adjustment in three positions: Δh_1, Δh_2, or Δh_3 (Figure 3C).

Regarding the methodological limits tested in the DP for the K_{sat} tests, both in the CHP and FHP methods, an evaluation was conducted to ascertain the sensitivity of the permeameter in detecting changes in the results depending on the hydraulic head applied (constant and falling) to the cylinder-sample sets (100 and 250 cm^3).

In the case of utilizing DP as CHP (Figure 3B), two values of h were defined: 1.5 and 2.5 cwc. The data generated in these tests were employed to calculate K_{sat} based on Darcy's Law using equation (5), as proposed by Reynolds and Elrick (1986).

$$K_{sat} = \left(\frac{Wv}{A\ t} \times \frac{L}{L+h}\right) \times 10 \quad (5)$$

where: K_{sat} is expressed in cm h^{-1}; Wv = volume of water collected (cm^3); L = height of the specimen (cm), assumed as the height of the volumetric cylinder used in sampling; A = cross-sectional area of the specimen, considered as the cylinder cross-sectional area ($\pi\ r^2$), expressed in cm^2; t = water flow time through the specimen (hours); and h = hydraulic head applied to the soil top (pressure potential: ϕ_p), expressed in centimeter of water column (cwc).

Conversely, when the DP was utilized as the FHP method, the cylinder-sample sets were subjected to three hydraulic heads that decreased in intensity between positions h_1 and h_2 (Figure 3C). To this end, three scenarios were analyzed: (i) Upper Limit (UL), defined by the maximum height of h_1, represented by the greatest distance between the meniscus of the burette (0 mL) and the base of the sample in the cylinder (reference level – RL); (ii) Medium Limit (ML), where the height of h_1 was fixed approximately to the center of the burette, with h_1 represented by the intermediate distance between the burette meniscus and the reference level (RL); iii) Lower Limit (LL) was defined by the smallest height of h_1, represented by the smallest distance between the burette meniscus and the RL. In each case, the position of h_2 was maintained at the value corresponding to a differential height of 10 cm. The time required for the water column to traverse the distance between h_1 and h_2 was also recorded, yielding the differential time (Δt). Therefore, the values of h_1 and h_2 for each Δh were as follows: Δh_i (UL), h_1 = 67.6 cwc and h_2 = 57.6 cwc; Δh_{ii} (ML), h_1 = 49.3 cwc and h_2 = 39.3 cwc; and Δh_{iii} (LL), with h_1 = 31.3 cwc and h_2 = 21.3 cwc.

According to the aforementioned conditions, the outcomes yielded by the tests were employed in the calculation of the K_{sat} values, utilizing the equation (6) put forth by Reynolds and Elrick (1986).

$$K_{sat} = \left[\frac{a\ L}{A\ \Delta t} \times \ln\left(\frac{h_1}{h_2}\right)\right] \times 10 \quad (6)$$

where: K_{sat} is expressed in mm h^{-1}; a = cross-sectional area of the graduated tube (cm^2); A = cross-sectional area of the specimen (cm^2); L = height of the specimen (cm), assumed as the height of the volumetric cylinder used in sampling; Δt = time interval of water flow through the specimen between h_1 and h_2, expressed in hours; h_1 = initial height of the water meniscus in the burette at the reference level (RL, located at the base of the sample), expressed in cm; h_2 = final height of the water meniscus in the burette at RL (cm).

Statistical analysis

Statistical analysis of the results obtained in scientific research is a crucial tool for validating these data and for the appropriate extrapolation of the results obtained for the studied population. In this context, the data were subjected to statistical analysis in a factorial scheme, to carry out an analysis of the research in question. This analysis was conducted separately for the CHP and FHP methods. In the case of the CHP, three factors were taken into consideration, namely the two volumes of soil samples (100 and 250 cm^3), five categories of soil horizons (P1-Ap, P1-Bt_1, P2-Ap, P3-Ap, and P3-Bt_1), with two constant hydraulic heads (1.5 and 2.5 cwc) and 20 replications. In the case of the FHP method, three factors were taken into consideration, namely two volumes of soil samples (100 and 250 cm^3), five soil horizons (P1-Ap, P1-Bt_1, P2-Ap, P3-Ap, and P3-Bt_1), and three hydraulic heads: a) falling hydraulic head applied with Δh_i = Upper Limit, where h_1 = 67.6 cwc and h_2 = 57.6 cwc; b) falling hydraulic head applied with Δh_{ii} = Medium Limit, where h_1 = 49.3 cwc and h_2 = 39.3 cwc, and c) falling hydraulic head applied with Δh_{iii} = Lower Limit, where h_1 = 31.3 cwc and h_2 = 21.3 cwc was determined in ten repetitions. The coefficients of variation were calculated to ascertain the degree of variability associated with the two methods of determining K_{sat} (CHP and FHP). The classification of this variability was conducted according to the recommendations proposed by Warrick and Nielsen (1980), who proposed the delineation of three distinct categories: low (CV < 12%), medium (12% < CV < 60%), and high (CV > 60%).

Results and Discussion

Hydraulic conductivity of saturated soil and its relationship with other physical attributes

It is generally observed that in tests with DP in the CHP method, the increase in the hydraulic head (ϕ_p from 1.5 to 2.5 cwc) did not increase K_{sat} values (Table 2), irrespective of the sample volume employed in the tests (100 and 250 cm^3). However, a comparison of the mean values between volumes (Table 2, capital letters in red) revealed that the samples with 250 cm^3 exhibited the highest values (26.16 mm h^{-1}), while those with 100 cm^3 demonstrated the lowest (8.17 mm h^{-1}). This phenomenon can be attributed to the average K_{sat} value of P3-Ap (123.50 mm h^{-1}), which elevated the mean of the set of samples with 250 cm^3 (26.16 mm h^{-1}). Notably, the P3-Ap sample is the only one with a sandy texture (916.49 g kg^{-1}), exhibiting high permeability via macropores with the increase due to preferential flow in samples with greater volume, as observed in other studies (Nimmo, 2021; Liu et al., 2023).

The mean K_{sat} values obtained in samples with 100 cm^3 volume, across all horizons, were found to be lower in comparison to samples with 250 cm^3 volume (Table 2). Therefore, when evaluating the impact of the head on each sample volume, it is observed that there was no discernible difference in the mean values obtained in the samples with 100 cm^3 when comparing the heads of 1.5 and 2.5 cwc (8.07 and 8.26 mm h^{-1}). In samples with a volume of 250 cm^3, the mean hydraulic head of 1.5 cwc was observed to be lower (25.35 mm h^{-1}) in comparison to the 2.5 cwc head (26.96 mm h^{-1}). Conversely, when K_{sat} was determined using DP in the FHP method (Table 3), the application of an increased hydraulic head did not affect the results for the two sample volumes tested (100 and 250 cm^3), regardless of the limit used (Δh).

Regarding the mean K_{sat} values for each volume (as detailed in the final column of Table 3), it is notable that, in contrast to the CHP method, the results for the FHP method in samples with 100 cm^3 were the highest (18.17 mm h^{-1}), while for 250 cm^3, there was a notable reduction to 7.28 mm h^{-1}.

The mean K_{sat} values obtained across all horizons remained consistent regardless of the tested limits of the applied hydraulic head (Δh_i, Δh_{ii}, and Δh_{iii}), irrespective of the sample volume (Table 3).

Table 2. Mean values of hydraulic conductivity in saturated soil (K_{sat}) obtained by the double constant-head permeameter (CHP), using samples collected in cylinders with volumes of 100 and 250 cm^3. Statistical analysis performed with data transformed into $x^{-0.03}$.

Sample volume (cm^3)	Horizon	Textural class	CHP: Applied hydraulic head (cwc) 1.5	CHP: Applied hydraulic head (cwc) 2.5	K_{sat} mean values (mm h^{-1}): Horizon	K_{sat} mean values (mm h^{-1}): Volume
100	P1-Ap	Sandy loam	15.93 aA*A*	14.71 aA*A*	15.32 A*A*	8.17 *B*
	P1-Bt_1	Clay loam	1.96 aB*A*	2.31 aB*A*	2.14 B*A*	
	P2-Ap	Sandy clay loam	12.21 aA*A*	11.76 aA*A*	11.99 A*A*	
	P3-Ap	Sandy	8.37 aA*A*	9.34 aA*B*	8.86 A*B*	
	P4-Bt_1	Sandy clay loam	1.89 aB*A*	3.20 aAB*A*	2.55 B*A*	
Volume mean with 100 cm^3			8.07 a*B*	8.26 a*B*		
250	P1-Ap	Sandy loam	0.62 aC*B*	1.08 *aCB*	0.85 C*B*	26.16 *A*
	P1-Bt_1	Clay loam	0.36 aC*B*	0.73 aC*A*	0.55 C*B*	
	P2-Ap	Sandy clay loam	0.73 bC*B*	1.34 aC*B*	1.04 C*B*	
	P3-Ap	Sandy	120.87 aA*B*	126.13 aB*A*	123.50 A*A*	
	P4-Bt_1	Sandy clay loam	4.16 aB*A*	5.54 aA*A*	4.85 B*A*	
Volume mean with 250 cm^3			25.35 b*A*	26.96 a*A*		
Total means			16.71 b	17.61 a		17.16

In each volume, the means followed by the same lowercase letter in the row and the same capital letter in the column do not differ by Tukey test at 5% significance. Among the volumes, means followed by the same italic capital letter in the column do not differ according to the Tukey test at 5% significance.

Table 3. Mean values of hydraulic conductivity in saturated soil (K_{sat}) obtained by the double falling-head permeameter (FHP), using samples collected in cylinders with volumes of 100 and 250 cm^3. Statistical analysis performed with data transformed into $x^{0.03}$.

Sample volume (cm^3)	Horizon	Textural class	FHP – Applied hydraulic head (cwc)			K_{sat} mean values (mm h^{-1})	
			Δhi^a	$\Delta h_{ii}{}^b$	$\Delta h_{iii}{}^c$	Horizon	Volume
100	P1-Ap	Sandy loam	49.83 aA*A*	49.07 aA*A*	75.38 aA*A*	58.09 A*A*	18.17 *A*
	P1-Bt_1	Clay loam	6.32 aC*A*	3.69 aC*A*	4.20 aC*A*	4.74 C*A*	
	P2-Ap	Sandy clay loam	11.28 aB*A*	12.08 aB*A*	16.37 aB*A*	13.24 B*A*	
	P3-Ap	Sandy	10.78 aBC*A*	10.01 aB*B*	14.12 aB*B*	11.64 B*B*	
	P4-Bt_1	Sandy clay loam	2.64 aD*B*	2.77 aC*B*	4.08 aC*B*	3.17 C*B*	
Volume mean with 100 cm^3			16.17 a*A*	15.52 a*A*	22.83 a*A*		
250	P1-Ap	Sandy loam	1.87 aC*B*	1.97 aC*B*	2.45 aB*B*	2.09 C*B*	7.28 *B*
	P1-Bt_1	Clay loam	1.27 aC*B*	1.42 aC*A*	1.41 aB*A*	1.37 C*B*	
	P2-Ap	Sandy clay loam	0.92 aC*B*	1.01 aC*B*	1.56 aB*B*	1.16 C*B*	
	P3-Ap	Sandy	19.64 aA*A*	23.61 aA*A*	29.50 aA*A*	24.25 A*A*	
	P4-Bt_1	Sandy clay loam	5.86 aB*A*	6.79 aB*A*	9.91 aA*A*	7.52 B*A*	
Volume mean with 250 cm^3			5.91 a*B*	6.96 a*B*	8.97 a*B*		
Total means			11.04 a	11.24 a	15.90 a		12.73

In each volume, the means followed by the same lowercase letter in the row and the same capital letter in the column do not differ by Tukey test at 5% significance. Among volumes, means followed by the same italic capital letter in the column do not differ according to the Tukey test at 5% significance. [a]Falling hydraulic head applied with Δh_i = Upper Limit, where h_1 = 67.6 cwc and h_2 = 57.6 cwc; [b]Falling hydraulic head applied with Δh_{ii} = Medium Limit, where h_1 = 49.3 cwc and h_2 = 39.3 cwc; and [c]Falling hydraulic head applied with Δh_{iii} = Lower Limit, where h_1 = 31.3 cwc and h_2 = 21.3 cwc.

The influence of the methods (CHP and FHP) on the K_{sat} outcomes can be elucidated by their dependence on specific variables, as previously observed and substantiated in the literature (Centeno et al., 2020; Liu et al., 2022). Indeed, K_{sat} is one of the physical water parameters of the soil that exhibits the highest coefficients of variation. Its values are markedly influenced by sample size, flow geometry, and the sample collection process (Bagarello and Provenzano, 1996; Soulis et al., 2020). Additionally, K_{sat} is affected by certain soil attributes, including soil bulk density, total porosity, distribution of particle size fractions, and others (Zeng et al., 2022).

The CHP method is recommended for highly permeable soils, such as those with a sandier texture. In contrast, the FHP method is more effective for low permeability soils, such as those from the most clayey classes (Mitchell-Fostyk and Haruna, 2021; Liu et al., 2022).

In addition to the necessity of maintaining the quality of the test specimen, the K_{sat} values are also contingent upon the selection of appropriate determination methods. Therefore, it is of paramount importance that the procedures conducted during the tests do not result in disturbances to the samples (Gonçalves and Libardi, 2013).

In this sense, it seems plausible to suggest that the utilization of double permeameter in the constant-head method for soils with a higher clay content, or in the falling-head method for those with a greater sand content, is a contributing factor to the discrepancies observed in the values obtained by the methods tested (CHP and FHP), as evidenced in Tables 2 and 3.

Table 4 illustrates the physical characterization of the profiles under examination, with particular emphasis on the values of soil bulk density (Bd), total porosity (TP), and particle size fractions. These attributes are of significant importance in discussions regarding their influence on the results of the K_{sat} values.

The results demonstrate that the Ap horizon of Profile 1 (Argissolo Amarelo eutrocoeso abrupto) exhibited the highest infiltration potential in comparison to the other horizons. This is attributed to its higher percentage of very coarse sand (VCS = 14.12%), combined with the lowest value of Bd (1.33 Mg m^{-3}) and higher TP (42.4%). The relationship between K_{sat} and these attributes has been documented by Haruna et al. (2018), who stated that the K_{sat} values are influenced by Bd, pore space, and connectivity, in addition to soil organic carbon (SOC) content. These results corroborate the higher K_{sat} values of Ap in relation to the other horizons (Table 2) when evaluating the smaller volume cylinder-sample sets (100 cm^3).

The cylinder-sample sets of the Bt_1 horizon of Profile 1 generally exhibited the lowest K_{sat} values (Tables 2 and 3). This horizon, despite its elevated total clay content (TC = 38.05%), exhibits the lowest proportion of water-dispersible clay (WDC = 0.41%) and, consequently, a heightened clay flocculation degree (FD ≅ 99%), in addition to elevated Bd (1.54 Mg m^{-3}), representing the second-highest observed value (Table 4). Therefore, the low K_{sat} in Bt_1 of Profile 1 can be attributed to its elevated FD, which is promoted by the greater quantity of kaolinite present in the profile. Consequently, in instances where the degree of Bt compaction is high, the resulting K_{sat} values are notably low. Moreover, the soil classification reveals its cohesive character, most pronounced in Bt_1, where the soil structure comprising kaolinite-type clay (Mota et al., 2021), disintegrates upon contact with water. It is therefore probable that deformation of the structure occurred during the tests, modifying the structural pores and thereby reducing the flow through these pores and the K_{sat} values.

Regarding Profile 2, Ap horizon, which is classified as a typical Argissolo Vermelho-Amarelo Distrocoeso, the most notable feature is its elevated level of water-dispersible clay (WDC = 163.01 g kg^{-1}), which consequently yields the highest value of clay dispersion degree - DD (≅ 73%) in comparison to the other horizons. Soils with high DD may have their pores blocked by dispersed clay, which can move during the saturation soil process, thereby reducing Ksat values during the tests (Awedat et al., 2021; Cruz et al., 2024).

The K_{sat} values were also found to be influenced by the size of the specimen, as observed by Šípek et al. (2019). The values were higher in samples with 100 cm^3 compared to those with 250 cm^3, except for the soil in Profile 3, Ap horizon (Tables 2 and 3).

Indeed, while the K_{sat} values of Profile 3, Ap horizon, classified as Argissolo Amarelo distrocoeso epiáquico, exhibit diminished fluctuations between the 100 cm^3 sample tests and the employed methods (Tables 2 and 3); however, this phenomenon was not observed for the 250 cm^3 sample. It was notable that the highest values were observed for the CHP method, with an average of 123.5 mm h^{-1}, in comparison to the values obtained by the FHP method, with an average of 24.3 mm h^{-1} (Table 4).

This phenomenon may be partially attributed to the preferential flow observed in sandy soil samples, which is enhanced when the sample size is increased (Liu et al., 2021; Nam et al., 2021).

In Profile 3, it is observed that the Ap horizon exhibited the highest concentration of total sand (916.49 g kg^{-1} ≅ 92 %), with this percentage predominantly distributed among the coarser subfractions (very coarse sand + coarse sand + medium sand), comprising 54.5% of the total soil composition. This proportion is the highest among the soils studied (Table 4).

Regarding the Bt_1 horizon of Profile 3, behavior contrary to that of the Ap horizon is observed, as it exhibits the lowest porosity (≅ 30%), reflecting its cohesive character, as evidenced by the highest Bd (1.67 Mg m^{-3}). This may account for the lower K_{sat} values among the studied soils (Tables 2, 3, and 4). The water dynamics observed in Profile 3 can be attributed, at least in part, to the distribution of total clay and sand (subfractions) within the Ap and Bt_1 horizons. The varying proportions of these fractions result in the formation of different pore sizes, including macro and micropores (Al-Kaisi et al., 2017; Parahyba et al., 2019). In this instance, the elevated sand values in the Ap horizon likely contributed to enhanced macroporosity, thereby facilitating greater soil drainage and aeration. This phenomenon can be attributed to the higher K_{sat} values observed in this horizon (Reichert et al., 2021). Indeed, as observed by Bisolo et al. (2024), macroporosity is directly proportional to the quantity of sand present in the soil, which consequently affects K_{sat} values. This direct correlation between macroporosity and soil K_{sat} is expected and is supported by the evidence that these properties derive from the same soil pore space (Jarvis et al., 2013; Karahan and Erşahin, 2017). Conversely, the lowest K_{sat} values in Bt_1 of Profile 3 may be associated with its total clay fraction (≅ 30%, the second highest among the soils), with a high FD (≅ 93%).

Table 4. Physical characterization of the studied profiles.

Horizon	Particle size distribution[1]									FD[8]	DD[9]	Pd[10]	Bd[11]	TP[12]
	Clay	Silt	Sand	VCS[2]	CS[3]	MS[4]	FS[5]	VFS[6]	CDW[7]					
	g kg^{-1}									%		Mg m^{-3}		%
Profile 1: Argissolo Amarelo eutrocoeso abrupto														
Ap	183.11	49.61	767.29	141.20	148.36	150.41	168.32	159.00	122.08	33.33	66.67	2.31	1.33	42.42
Bt_1	380.47	256.45	363.07	69.13	72.47	176.43	0.12	44.92	4.07	98.93	1.07	2.61	1.54	41.00
Profile 2: Argissolo Vermelho-Amarelo Distrocoeso típico														
Ap	224.13	7.76	768.11	132.94	168.39	147.22	198.53	121.03	163.01	27.27	72.73	2.47	1.45	41.30
Profile 3: Argissolo Amarelo distrocoeso epiáquico														
Ap	60.22	23.28	916.49	129.29	169.33	246.42	237.54	133.91	20.07	66.67	33.33	2.35	1.41	40.00
Bt_1	301.11	16.19	682.69	26.51	151.48	268.80	200.49	35.41	20.07	93.33	6.67	2.37	1.67	29.54

[1]Densimeter method (Almeida, 2008); [2]Very coarse sand; [3]Coarse sand; [4]Medium sand; [5]Fine sand; [6]Very fine sand; [7]Clay dispersed in water; [8]Degree of flocculation; [9]Degree of dispersion; [10]Soil solid particle density; [11]Soil density; [12]Total soil porosity.

However, high compaction conditions (Bd = 1.67 Mg m^{-3}), due to the cohesive character of the soil, contributed to greater microporosity, which reduced the infiltration rate in this horizon due to its greater water retention, as also observed in the findings of Reichert et al. (2021).

In consequence, Šípek et al. (2019) posit that K_{sat} values are contingent upon the dimensions and composition of the mineralogical constituents present within the soil, where minerals of a finer nature, such as silt and clay, have the potential to considerably reduce the values observed. Consequently, an examination of the K_{sat} results (Tables 3 and 4) reveals that the high degree of variation between the values can be attributed to the differing textures of the soils (Table 1). This variation can be attributed to the use of different standardization methods, such as the CHP or FHP. Bargarello and Provenzano (1998) demonstrated that K_{sat} results obtained using a laboratory permeameter are influenced by the size of the soil sample. They observed that samples of a larger size produced lower and less variable K_{sat} estimates than samples of a smaller size, which exhibited a greater potential for preferential flow. The findings of these authors may explain the differences in K_{sat} observed for Profile 2, Ap horizon (Tables 2 and 3), when determined in larger samples (250 cm^3). The permeameter used by Bargarello and Provenzano (1998) was of the traditional type, with artisanal assembly and separate saturation of the samples, which were then transferred to the permeameter.

These procedures have been demonstrated to disrupt the structural integrity of the sample, resulting in the formation of fissures and a preferential flow of water during the tests, which in turn elevates the K_{sat} value. This phenomenon has been corroborated by previous studies (Gonçalves and Libardi, 2013; Nam et al., 2021). These points were observed differently in this study because the samples were not influenced by preferential flow, as they received minimal disturbance during the equipment assembly and sample saturation. In particular, the saturation was conducted with the equipment already assembled with the specimen, which helped to ensure minimal disturbance.

In the case of the results presented in Table 3, the laboratory permeameter utilized in the tests is a device that employs saturation procedures and the determination of the infiltration rate within the apparatus itself, obviating the necessity for handling the sample throughout the process, even when a change in method is required, such as alternating between the CHP and FHP methods. These findings justify the higher K_{sat} values observed in samples collected in cylinders with a volume of approximately 100 cm^3 (Table 3).

Considering the aforementioned considerations, it is pertinent to inquire whether the justifications can be applied to the data presented in Table 4, which employs a larger sample size. The answer to this question hinges on the disruption of the sample, which results in the loss of its original structure.

Coefficient of variation

The coefficient of variation (CV) was employed to evaluate the performance of DP in estimating K_{sat}. To that end, all variables involved in the trials were considered, including sample size, constant hydraulic head, falling hydraulic head, and types of horizons studied. The results of this analysis can be seen in Table 5. The CV values for K_{sat} exhibited variability classified as medium (12% < CV < 60%) to high (> 60%), as proposed by Warrick and Nielsen (1980). The highest values were generally observed for the K_{sat} tests conducted on samples from Profile 1, Ap horizon, via the FHP method, irrespective of the sample size and the falling head applied, ranging between 119 and 156%.

The high CV values for the hydraulic conductivity of soils have been widely publicized in the literature. The high spatial variability of this physical-water attribute is ascribed to the numerous factors that influence its results, including the current soil moisture during the *in situ* tests (Gunaratnam et al., 2020), as well as biological activity, such as the growth and decay of roots and the activity of soil fauna, which, in turn, affects soil bulk density and total porosity, as demonstrated by Šípek et al. (2019).

Table 5. Coefficients of variation (CV) for K_{sat} results for soils via double permeameter, volumetric cylinders of 100 cm^3 and 250 cm^3, using the CHP method under hydraulic heads of ϕ_{p1} = 1.5 cwc and ϕ_{p2} = 2.5 cwc, and the FHP method applying hydraulic head variation under the upper, medium, and lower limits.

Permeameter type	Sample size	Applied hydraulic head	Profile 1		Profile 2	Profile 3	
			Ap	Bt_1	Ap	Ap	Bt_1
	__ cm^3 __	__ cwc __	CV (%)				
CHP	100	ϕ_{p1} = 1.5	61.19	123.34	59.80	109.69	87.60
		ϕ_{p2} = 2.5	61.67	102.62	57.31	92.30	79.19
	250	ϕ_{p1} = 1.5	113.51	103.10	144.47	68.54	142.46
		ϕ_{p2} = 2.5	96.22	87.64	110.73	65.41	107.14
FHP	100	UL	156.03	85.40	193.20	70.86	135.29
		ML	137.46	82.83	133.73	103.39	94.97
		LL	142.85	94.52	120.77	158.07	88.64
	250	UL	119.11	113.68	107.05	19.89	32.77
		ML	122.90	118.17	111.56	23.54	31.44
		LL	122.54	109.48	111.20	46.36	26.69

UL: Upper limit, where h_1 = 67.6 cwc and h_2 = 57.6 cwc; ML: Medium limit, where h_1 = 49.3 cwc and h_2 = 39.3 cwc; LL: Lower limit, where h_1 = 31.3 cwc and h_2 = 21.3 cwc.

Accordingly, Bisolo et al. (2024) ascribed the elevated K_{sat} coefficient of variation to the local effect, attributable to the pronounced spatial variability of soils, a phenomenon commonly observed in the three-dimensional movement properties of water. Abreu et al. (2004) observed a CV of 53%, respectively, for the K_{sat} values obtained in the field. As stated by Elrick and Reynolds (1992), the coefficient of variation can reach 300% in clayey soils. Lima et al. (2006) observed a CV between 112 and 248%.

In general, the most optimal performance was observed for tests with samples from Profile 3, Ap horizon, predominantly in the CHP and FHP methods, 250 cm^3 cylinders, irrespective of the applied hydraulic head. In this instance, the lowest values of heads observed for FHP were 19.89, 23.54, and 46.36% for the upper (UL), medium (ML), and lower (LL) limits, respectively. As for CHP, the values were 68.54% and 65.41%, respectively, for hydraulic heads of ϕ_{p1} = 1.5 cwc and ϕ_{p1}= 2.5 cwc (Table 5).

The lower CV values observed in the tests with Profile 3, Ap horizon, using falling heads suggest that the DP is dependent on the sample size. This indicates that the tests performed on the sample with 250 cm^3 exhibited superior performance. These findings were also observed in other studies. For instance, Almeida et al. (2017) analyzed the effect of different cylinder sizes (≅ 98 cm^3 and ≅ 312 cm^3) on K_{sat} results with the CHP and FHP methods and found that the results for tests with the CHP method, a larger cylinder, showed a lower CV, indicating better representation of the samples.

At this scale level, with sample sizes for K_{sat} tests in the laboratory (100 and 250 cm^3), it can be inferred that the results are dependent on the sample size. Indeed, other studies with a broader size range have already corroborated this trend. In this regard, Putera et al. (2013) conducted K_{sat} tests with the FHP method and observed that samples with smaller diameters (≤ 3" ≅ ≤ 7.62 cm × 1 cm in height, volume ≅ 46 cm^3) may not represent field conditions in comparison to the samples with a larger diameter (10" ≅ 25.4 cm × 8 cm in height, volume ≅ 4000 cm^3), where an increase in sample size has been shown to result in significant changes in K_{sat} values. Other authors have demonstrated the significant variability of K_{sat} as a function of sample size at the field scale. In this regard, Lanoix et al. (2020) evaluated the determination of *in situ* hydraulic conductivity in sandy soil using a single-ring infiltrometer, a double-ring infiltrometer, and a Guelph permeameter. The authors reported on the effect of ring size when tests were conducted using the single-ring method (SR). The authors observed that when the SR with a larger diameter (30 cm) was utilized, the K_{sat} values were typically lower than those obtained from the smaller ring tests (15 cm). This observed discrepancy between the action radiuses of the rings serves to corroborate the assertion that the tests conducted with a larger infiltrometer radius were less susceptible to boundary conditions and lateral water flow and thus were deemed more indicative of vertical infiltration. Consequently, the considerable variability in K_{sat} values is not only evident in the data generated in the laboratory but also in field tests (Fiori et al., 2010).

Field methods are more recommended for determining K_{sat}, as they cover a larger volume of soil and allow for the assessment of the effects of natural variability and soil discontinuities, in addition to not requiring the removal of deformed or undisturbed soil samples (Fiori et al., 2010). Conventional methods require a greater number of tests to generate significant data (Oliveira et al., 2021), which can burden the process of obtaining *in situ* results in terms of duration and cost (Strayer et al., 2003; Black, 2010).

Laboratory tests also have inherent difficulties and uncertainties, including those related to the scale factor. This is because the flow is evaluated in smaller volumes of soil (*e.g.*, volumetric cylinders of 100 and 250 cm^3), which may still present problems with obtaining sample numbers that are representative for estimating K_{sat} (Gootman et al., 2020). Moreover, as previously stated, there are challenges in maintaining the sample structure throughout the tests, selecting methods (CHP or FHP), as well as in acquiring automated commercial permeameters, which are costly (Feki et al., 2020; Zhao et al., 2023).

Considering these considerations, the DP exhibited several advantageous characteristics. Primarily, it demonstrated an effective reduction in issues associated with the disruption of the sample structure, particularly in the context of sandy soils. Additionally, the fabrication of the DP entailed minimal costs, as it was constructed using readily accessible materials, with a relatively short production time.

Conclusions

The results generated by the laboratory tests for determining K_{sat} values using the double permeameter allowed to conclude that:

- The tests for determining K_{sat} using the CHP and FHP methods, while keeping the sample fixed to the same position, did not cause any disturbance to the soil structure;
- The hydraulic head applied to the soil during laboratory tests, using the CHP method, did not influence the K_{sat} values obtained by the double permeameter. This allowed for the use of values between 1.5 cwc and 2.5 cwc;
- The sample size influenced the results obtained for K_{sat} by the double permeameter, which were larger for the samples considered standard (100 cm^3) than for those collected in the volumetric cylinders with 250 cm^3;
- The double permeameter can be used within the methodological limits applied in this study, with the limit being selected according to the physical properties of the soils to be used in the tests and the availability and construction of the equipment and apparatus.

Acknowledgments

This study was partly financed by the Coordenação de Aperfeiçoamento de Pessoal de Nível Superior - Brasil (CAPES) - Finance Code 001. The authors declare no conflict of interest.

References

Abreu, S.L., Reichert, J.M., Reinert, D.J. 2004. Escarificação mecânica e biológica para a redução da compactação em Argissolo franco-arenoso sob plantio direto. Revista Brasileira de Ciência do Solo 28, 519-531. http://dx.doi.org/10.1590/S0100-06832004000300013

Almeida, B.G., Almeida, C.D.G.C., Santos, E.M.S., Maia, A.J., Silva, T.H.S. 2020. Permeâmetro contínuo de carga constante e decrescente para determinação de condutividade hidráulica em meios porosos (Patente brasileira nº BR1020200132024). Instituto Nacional da Propriedade Industrial.

Almeida, K.S.S.A., Souza L.S., Paz, V.P.S., Silva, F.T.S., Santos, D.N., Pereira, J.S.L. 2017. Variabilidade espacial da condutividade hidráulica do solo saturado em latossolo amarelo distrocoeso, no município de Cruz das Almas. Irriga 22 (2). http://dx.doi.org/10.15809/irriga.2017v22n2p259-274

Awedat, A.M., Zhu, Y., Bennett, J.M., and Raine, S.R. 2021. The impact of clay dispersion and migration on soil hydraulic conductivity and pore networks, Geoderma 404, 115297. https://doi.org/10.1016/J.GEODERMA.2021.115297, 2021.

Bagarello, V., Provenzano, G. 1996. Factors affecting field and laboratory measurement of saturated hydraulic conductivity. Transactions of the ASAE 39 (1), 153-159. https://doi.org/10.13031/2013.27493

Bisolo, A., Rodrigues, M., Conceição, F., Pellegrini, A. 2024. Spatial variability and correlation between soil physical properties under no-tillage with and without agricultural terraces. Brazilian Archives of Biology and Technology 67, e24230802, 1-13. https://doi.org/10.1590/1678-4324-pssm-2024230802

Black, J.H. 2010. The practical reasons why slug tests (including falling and rising head tests) often yield the wrong value of hydraulic conductivity. Quarterly Journal of Engineering Geology and Hydrogeology 43 (3), 345-358. https://doi.org/10.1144/1470-9236/08-094.

Centeno, L.N., Timm, L.C., Reichardt, K., Beskow, S., Caldeira, T.L., Oliveira, L.M., Wendroth, O. 2020. Identifying regionalized co-variate driving factors to assess spatial distributions of saturated soil hydraulic conductivity using multivariate and state-space analyses. Catena 191, 104583. https://doi.org/10.1016/j.catena.2020.104583.

Cruz, D.L.S., Vale Júnior, J.F., Neves, L.T.C., Carvalho, L.B., Ahouangbonou, O.R.K. 2024. Soil physical quality: a comprehensive analysis of its importance for agricultural production. Revista Agro@mbiente On-line 18. e8060. http://dx.doi.org/10.18227/1982-8470ragro.v18i00.8060

Elrick, D.E., Reynolds, W.D. 1992. Methods for analyzing constant-head well permeameter data. Soil Science Society of America Journal 56 (1), 320-323. http://dx.doi.org/10.4067/S0718-27912008000100001.

Feki, M., Ravazzani, G., Barontini, S., Ceppi, A., Mancini, M. 2020. A comparative assessment of the estimates of the saturated hydraulic conductivity of two anthropogenic soils and their impact on hydrological model simulations. Soil and Water Research 15 (3), 135-147. https://doi.org/10.17221/33/2019-SWR

Ferdinand, A.M., Dorothée, D.B., Codjo, A.E. 2023. Experimental analysis of hydraulic conductivity for saturated granular soils. Geomaterials 13, 71-90. https://doi.org/10.4236/gm.2023.133006

Fiori, J.P.O., Campos, J.E.G., Almeida L. 2010. Variabilidade da condutividade hidráulica das principais classes de solos do estado de Goiás. Geociências 29 (2), 229-235.

Flint, A.L., Flint, L.E. 2002. Particle Density. In: Dane, J.H., Topp, G.C. Methods of soil analysis: Physical methods. Soil Science Society of America, Madison. Part 4. 229-241.

FAO. Food and Agriculture Organization of the United Nations. 2023. Standard operating procedure for soil bulk density, cylinder method. Rome. https://doi.org/10.4060/cc7568en

Gee, G.W., Or, D. 2002. Particle Size Analysis. In: Dane, J.H., Topp, G.C. Methods of soil analysis. Physical methods. Soil Science Society of America, Madison. Part 4. 255-293.

Gonçalves, A.D.M.A., Libardi, P.L. 2013. Análise da determinação da condutividade hidráulica do solo pelo método do perfil instantâneo. Revista Brasileira de Ciência do Solo [online] 37 (5), 1174-1184. https://doi.org/10.1590/S0100-06832013000500007. ISSN 0100-0683.

Gootman, K.S., Kellner, E., Hubbart, J.A. 2020. A comparison and validation of saturated hydraulic conductivity models. Water 12, 20-40. https://doi.org/10.3390/w12072040

Grossman, R.B., Reinsch, T.G. 2002. The solid phase. In Dane, J. H., Topp, G. C. (Eds.), SSSA Book Series: 5. Methods of Soil Analysis Part 4-Physical Methods. Soil Science Society of America Inc. Madison, WI, 201-415.

Gubiani, P. I., Reinert, D. J., Reichert, J. M., Gelain, N. S., Minella, J. P. G. 2010. Permeâmetro de carga decrescente associado a programa computacional para a determinação da condutividade hidráulica do solo saturado. Revista Brasileira de Ciência do Solo 34 (3). https://doi.org/10.1590/S0100-06832010000300041

Guedessou, C. V., Caron, J., Gallichand, J., Béliveau, M., Dessureault-Rompré, J., Libbrecht, C. 2021. Modeling subsurface drainage in compacted cultivated histosols. Frontiers in Water 2, 608910. https://doi.org/10.3389/frwa.2020.608910

Gunaratnam, A., Grafton, M., Jeyakumar, P., Bishop, P., Davies, C.E., Mccurdy, M. 2020. Study the influence of soil moisture and packing incremental level on soil physical and hydraulic properties. In: Nutrient Management in Farmed Landscapes. (Eds. C.L. Christensen, D.J. Horne and R. Singh). New Zealand. 6 p.

Haruna, S.I., Nkongolo, N.V., Anderson, S.H., Eivazi, F., Zaibon, S. 2018. In situ infiltration as influenced by cover crop and tillage management. Journal of Soil and Water Conservation 73, 164–172. https://doi.org/10.2489/jswc.73.2.164.

Jarvis, N., Koestel, J., Messing, I., Moeys, J., Lindahl, A. 2013. Influence of soil, land use and climatic factors on the hydraulic conductivity of soil. Hydrology and Earth System Sciences 17, 5185-5195. https://doi.org/10.5194/hess-17-5185-2013.

Karahan, G. K., Erşahin, S. 2017. Relating macropore flow to soil parametric and morphological variables. Soil Science Society of America Journal 81 (5), https://doi.org/10.2136/sssaj2016.10.0327

Lanoix, M.L., Pabst, T., Aubertin, M. 2020. Field determination of the hydraulic conductivity of a compacted sand layer controlling water flow on an experimental mine waste rock pile. Hydrogeology Journal 28, 1503–1515. https://doi.org/10.1007/s10040-020-02129-7

Liao, K., Feng, J., Lai, X., Zhu, Q. 2022. Effects of environmental factors on the influence of tillage conversion on saturated soil hydraulic conductivity obtained with different methodologies: a global meta-analysis. SOIL 8, 309–317. https://doi.org/10.5194/soil-8-309-2022

Lima, C.L.R., Reinert, D.J., Reichert, J.M., Suzuki, L.E.A.S., Gubiani, P. I. 2006. Qualidade físico-hídrica e rendimento de soja (*Plycine max L.)* e feijão (*Phaseolus vulgaris L.)* de um argissolo vermelho distrófico sob diferentes sistemas de manejo. Ciência Rural 36 (4). https://doi.org/10.1590/S0103-84782006000400020.

Liu, J., Xu, Q., Li, P., He, P., Pu, C., Zhao, K., Peng, D., Wang, Z. 2022. Saturated permeability of compacted loess based on low-field nuclear magnetic resonance (NMR). Bulletin of Engineering Geology and the Environment 81, https://doi.org/10.1007/s10064-022-02955-x

Liu, L., Liu, X., Yao, Y., Qi, W., Guo, Y. 2023. Preferential flow in the understory soil of *Hippophae rhamnoides* at different stump heights. Frontiers in Environmental Science 11, 1183448. https://doi.org/10.3389/fenvs.2023.1183448

Liu, Y.; Zhang, Y.; Xie, L.; Zhao, S.; Liyi, D.; Zhang, Z. 2021. Effect of soil characteristics on preferential flow of Phragmites australis community in Yellow River delta. Ecological Indicators 125, 107486. https://doi.org/10.1016/j.ecolind.2021.107486

Mitchell-Fostyk, B.A., Haruna, S.I. 2021. Spatial and fractal characterization of soil hydraulic properties along a catena. Soil Soil Science Society of America Journal 85, 1710–1726. https://doi.org/10.1002/saj2.20286.

Mota, J.C.A., Silva, C.P., Almeida, B.G., Romero, R.E., Alencar, T.L., Lobato, M.G.R., Oliveira, L.S., Souza, L.S., Costa, M.C.G. 2021. Cohesive character in Alfisols, Ultisol and Oxisols in Northeast of Brazil: Relationship of tensile strength with silicon, aluminum and iron from poorly crystalline compounds. Geoderma Regional 24, e00361. https://doi.org/10.1016/j.geodrs.2021.e00361.

Nam, S., Gutierrez, M., Diplas, P., Petrie, J. 2021. Laboratory and in situ determination of hydraulic conductivity and their validity in transient seepage analysis. Water 13 (8), 1131. https://doi.org/10.3390/w13081131

Nimmo, J. 2021. The processes of preferential flow in the unsaturated zone. Soil Science Society of America Journal 85 (1). https://doi.org/ 10.1002/saj2.20143.

Oliveira, M. E. D., Gastmans, D., Sacchi, M. D., Rocha, R. E., Lima, C., Santos, V. 2021. Determining a composite value for the saturated hydraulic conductivity in a recharge area of the Guarani Aquifer System, using pedotransfer functions. Revista Brasileira de Recursos Hídricos 26 (35). https://doi.org/10.1590/2318-0331.262120210045

Parahyba, R.B.V, Araújo, M.S.B., Almeida, B.G., Rolim Neto, F.C., Sampaio, E.V.S.B., Caldas, A.M. 2019. Water retention capacity in Arenosols and Ferralsols in a semiarid area in the state of Bahia, Brazil. Anais da Academia Brasileira de Ciências 91, e20181031. https://doi.org/10.1590/0001-3765201920181031

Putera, A.M.A, Damianto, B., Pramusandi, S. 2013. Hydraulic conductivity measurement of compacted clay soil liners for waste containment structures. Journal of Earth Sciences and Geotechnical Engineering 3 (4), 125-145. ISSN: 1792-9040 (print), 1792-9660 (online)

Reichert, J.M., Fontanela, E., Awe, G.O., Fasinmirin, J.T. 2021. Is cassava yield affected by inverting tillage, chiseling or additional compaction of no-till sandy-loam soil? Revista Brasileira de Ciência do Solo 45, e0200134. https://doi.org/10.36783/18069657rbcs20200134

Reynolds, W.D., Bowman, B.T., Brunke, R.R., Drury, C.F., Tan, C.S. 2000. Comparison of tension infiltrometer, pressure infiltrometer, and soil core estimates of saturated hydraulic conductivity. Soil Science Society of America Journal 64, 478-484 https://doi.org/10.2136/sssaj2000.642478x.

Reynolds, W.D., Elrick, D.E. 1986. A method for simultaneous in situ measurement in the vadose zone of field-saturated hydraulic conductivity, sorptivity and the conductivity pressure head relationship. Ground Water Monitoring Review 6, 84-95.

Santos, H.G., Jacomine, P.K.T., Anjos, L.H.C., Oliveira, V.A., Lumbreras, J.F., Coelho, M.R., Almeida, J.A., Araújo Filho, J.C., Oliveira, J.B., Cunha, T.J.F. 2018. Sistema brasileiro de classificação de solos. 5ed. Embrapa, Brasília, DF, p.531 rev. e ampl. ISBN 978-85-7035-800-4.

Šípek, V., Jačka, L., Seyedsadr, S., Trakal, L. 2019. Manifestation of spatial and temporal variability of soil hydraulic properties in the uncultivated Fluvisol and performance of hydrological model. Catena 182, 104119. https://doi.org/10.1016/j.catena.2019.104119

Snoussi, G., Nasri, B., Hamdi, E., Fouché, O. 2024. Reuse of Tunisian excavated material into composite soil for rainwater infiltration within urban green infrastructure. Geoderma Regional 36, e00748. https://doi.org/10.1016/j.geodrs.2023.e00748

Solangi, K., Abbasi, B., Solangi, F., Khaskhali, S., Siyal, A.A., Mehmood, H., Akram, M., Iqbal, R., Al-Ghamdi, A., Elshikh, M. 2024. Assessment of saturated hydraulic conductivity with using soil particle size distribution: a comparative study of constant head and falling head methods. Global NEST Journal 26 (6), 05833. https://doi.org/10.30955/gnj.005833

Soulis, K.X., Londra, P.A., Kargas, G. 2020. Characterizing surface soil layer saturated hydraulic conductivity in a Mediterranean natural watershed. Hydrological Sciences Journal 65 (15), 2616-2629. https://doi.org/10.1080/02626667.2020.1831694.

Strayer, D.L., Beighley, R.E., Thompson, L.C., Brooks, S., Nilsson, C., Pinay, G., Naiman, R.J. 2003. Effects of land cover on stream ecosystems: roles of empirical models and scaling issues. Ecosystems 6, 407-423. https://doi.org/10.1007/PL00021506

Su, W., Cui, Y.J., Zhang, F., Ye, W. 2020. Revisiting the methods of determining hydraulic conductivity of saturated expansive clays in low-compressibility zone. Journal of Rock Mechanics and Geotechnical Engineering 12 (5), 1131-1136. https://doi.org/10.1016/j.jrmge.2020.01.004

Warrick, A.W., Nielsen, D.R. 1980. Spatial variability of soil physical properties in the field. In: Hillel, D. (Ed.). Applications of soil physics. New York: Academic. p, 319-344.

Zeng, Z., Xia, J., Dong, S., Cai, W., Chuanbin, D., Liu, X., Zu, J., Zhu, X., Yang, L. 2022. Spatial variation of saturated hydraulic conductivity in a riparian zone: A case study of the Baoan Lake in Hubei Province, China. Catena 210, 105891. https://doi.org/10.1016/j.catena.2021.105891.

Zhao, W., Wang, M., Chen, C., Huang, L. 2023. Variations, controls and predictions of soil saturated hydraulic conductivity under different land use types in the alpine region of Tibet, China. Geoderma Regional 35, e00723. https://doi.org/10.1016/j.geodrs.2023.e00723

Yan, X., Zhou, W., Zhang, Y., Zuo, C., Cheng, Q. 2024. Estimating near-surface soil hydraulic properties through sensor-based soil infiltrability measurements and inverse modeling. Forests 15, 569. https://doi.org/10.3390/f15030569